HHS Public Access

Author manuscript

Anesthesiology. Author manuscript; available in PMC 2016 August 01.

Published in final edited form as:

Anesthesiology. 2015 August ; 123(2): 346–356. doi:10.1097/ALN.0000000000000731.

Resting State Functional Magnetic Resonance Imaging Correlates of Sevoflurane-induced Unconsciousness

Ben Julian A. Palanca, M.D., Ph.D., M.Sc.[a] **[Assistant Professor]**, **Anish Mitra, MS**[b] **[Graduate Student]**, **Linda Larson-Prior, Ph.D.**[b,d] **[Associate Professor]**, **Abraham Z. Snyder, M.D, Ph.D.**[b,d] **[Research Professor]**, **Michael S. Avidan, M.B.B.Ch.**[a,c] **[Professor]**, and **Marcus E. Raichle, M.D.**[b,d,e,f] **[Professor]**

[a]Department of Anesthesiology, Washington University School of Medicine in St. Louis

[b]Department of Radiology, Washington University School of Medicine in St. Louis

[c]Department of Surgery, Division of Cardiothoracic Surgery, Washington University School of Medicine in St. Louis

[d]Department of Neurology, Washington University School of Medicine in St. Louis

[e]Department of Anatomy and Neurobiology, Washington University School of Medicine in St. Louis

[f]Department of Biomedical Engineering, Washington University in St. Louis

Abstract

Background—Blood oxygen level dependent (BOLD) functional magnetic resonance imaging (fMRI) has been used to study the effects of anesthetic agents on correlated intrinsic neural activity. Prior studies have focused primarily on intravenous agents. We studied the effects of sevoflurane, an inhaled anesthetic.

Methods—Resting state BOLD fMRI was acquired from ten subjects before sedation and from nine rendered unresponsive by 1.2% sevoflurane. The fMRI data were analyzed taking particular care to minimize the impact of artifact generated by head motion.

Results—BOLD correlations were specifically weaker within the default mode (DMN) and ventral attention network (VAN) during sevoflurane-induced unconsciousness, especially between anterior and posterior midline regions. Reduced functional connectivity between these same networks and the thalamus were also spatially localized to midline frontal regions. The amplitude of BOLD signal fluctuations was substantially reduced across all brain regions. The importance of censoring epochs contaminated by head motion was demonstrated by comparative analyses.

Conclusions—Sevoflurane-induced unconsciousness is associated both with globally reduced BOLD signal amplitudes and with selectively reduced functional connectivity within cortical networks associated with consciousness (DMN) and orienting to salient external stimuli (VAN).

Corresponding Author: Palanca, Ben Julian Agustin, Wash University School of Medicine, Department of Anesthesiology, 660 S. Euclid Avenue, Box 8054, St. Louis, MO 63110 USA, Phone: 314-362-1196, Fax: 314-747-3977, palancab@wustl.edu. Department of Anesthesiology, Washington University School of Medicine in St. Louis

Competing Interests: The authors declare no competing interests.

Scrupulous attention to minimizing the impact of head motion artifact is critical in fMRI studies employing anesthetic agents.

Introduction

Anesthetic agents induce profound derangements of consciousness and cognition. The neural mechanisms underlying sedation and general anesthesia include potentiation and inhibition of target receptors and ion channels[1] and modulation of subcortical arousal circuitry.[2] Electrophysiological recordings have also implicated disrupted signaling between distant brain regions.[3,4] At the systems level, functional magnetic resonance imaging (fMRI) provides a means of elucidating mechanisms whereby humans rendered unconscious fail to perceive, attend, or react to the external world.

Functional magnetic resonance imaging is based on the measurement of blood oxygen level dependent (BOLD) signals[5] that indirectly reflect neural activity.[6] Task-based fMRI has been extensively used to localize sensory, motor and cognitive functions to specific patterns of activated brain regions.[7] More recently, task-free ("resting state") fMRI has been used to probe this neural architecture in diverse cognitive states.[8] Resting state fMRI exploits the fact that intrinsic activity is temporally coherent within widely distributed functional systems.[9] This phenomenon is referred to as functional connectivity (FC); the associated topographies comprise resting state networks (RSNs).[10] RSNs are associated with specific functions based on the observation that their topographies recapitulate fMRI responses to task paradigms.[11,12]

Reports describing human resting state fMRI effects of sedation date back to 2000[13] and now number several dozen, listed as a table with study parameters in Supplemental Digital Content 1. Loss of purposeful responses to verbal or painful stimulation has been associated with reversible disruption of FC within RSNs.[14–16] Most prior studies in this field used intravenous agents, primarily propofol. In contrast, sevoflurane has been less often used and some of the reported effects are inconsistent with the rest of the literature. For example, whereas reduced FC within the default mode network (DMN) is a commonly observed correlate of propofol-induced unconsciousness,[14,16] Martuzzi and colleagues studied 1% sevoflurane and did not observe this effect.[17] It is unclear whether this discrepancy reflects pharmacologic differences between anesthetic agents or technical confounding factors such as motion artifact. The extent to which micro-movements of the head contribute to spurious FC findings has been recognized only recently.[18–22] Since the bulk of fMRI investigations on anesthetic-induced unconsciousness were conducted prior to quantitative censoring of motion artifact, it is unknown what effect this potential confound has had on the body of knowledge in this field.

Here, we report a resting state fMRI study of the unconsciousness induced by sevoflurane, incorporating scrupulous attention to minimizing the impact of head motion-related artifact. We hypothesized that sevoflurane-induced unconsciousness would reduce FC, particularly within the default mode network.[15,23–25] We also demonstrate that head motion is a significant source of artifact in studies of this type, and can produce false effects in both the correlation and covariance structure of resting state fMRI.

Materials and Methods

Study Participants

All aspects of this study were supervised by the Washington University Human Research Protection Office, including regular review by a data monitoring and safety board. Inclusion criteria included: 18 to 40 years of age, American Society of Anesthesiologists Physical Status Class I, body mass index of 18–30 kg/m^2. Exclusion criteria included: use of over-the-counter antihistamines, anti-emetics, herbal supplements, ethanol, or illicit drugs within a week of the study; known auditory or physical impairments; known family history of malignant hyperthermia; sedation, general anesthesia, or upper respiratory infection in the past 30 days; disturbance in normal sleep pattern within the past 14 days, or implanted MRI-incompatible metal or prosthetic. In total, 224 applicants were screened. Of these, 43 participants were enrolled in the study. Eligible study volunteers underwent a history and physical examination Preparation for sedation involved overnight fasting. Female participants underwent urine pregnancy testing. All participants gave written informed consent and were paid for their participation. Functional imaging was initiated in 21 participants but aborted in 5 because of agitation manifesting as gross motion, vocalization, tachycardia, or hypertension.

Anesthetic Protocol

Sessions were carried out in the Center for Clinical Imaging and Research within Barnes-Jewish Hospital. At least one ACLS-certified anesthesiologist, research nurse, and MR technician were present throughout each imaging session. A forearm intravenous catheter provided fluid and drug access. A radial arterial catheter was placed for blood gas sampling. Invasive blood pressure, temperature, oxygen saturation, and end-tidal carbon dioxide and sevoflurane concentration were measured using a Medrad Veris monitoring system (Medrad Inc, Warrendale, PA). An airtight face-mask provided allowed administration of sevoflurane and exhaled gas monitoring during spontaneous breathing. Mask leaks were inferred from large gradients in inspired and expired oxygen percentages, capnographic traces, or noises from the masks. The RF coil and padding in front of the mask was used to secure the mask to the face of the participant. Gas administration was controlled through a Dräger Narkomed MRI-2 machine (Dräger North America). A mixture of 2 L/min air: 2 L/min oxygen was delivered throughout the study.

The experimental protocol involved step-wise changes in inhaled sevoflurane concentration, from 0% to 1.2% and back to 0%, in 0.6% increments, with a goal of deep sedation at 0.6% sevoflurane and unconsciousness at 1.2% (0.6–0.7 minimum alveolar concentration, MAC[26]). After each step, fifteen minutes of anesthetic equilibration were allotted before functional BOLD imaging data were acquired. Excessive subject motion at 0.6% sevoflurane precluded analysis of fMRI data acquired at this concentration. Hence, we report only fMRI data acquired at baseline (0%) and 1.2% sevoflurane. Arterial blood gases, for measuring arterial carbon dioxide partial pressure ($PaCO_2$), were sampled after at least twenty minutes of equilibration and were analyzed using a portable I-Stat and G3+ cartridges (Abbott Point of Care Inc., Princeton, NJ). Behavioral assessments were based on the modified Observer's Assessment of Alertness/Sedation Scale[27] and the Ramsay Sedation

Scale.[28] If verbal responses were not elicited, noxious pressure was applied to fingernail beds (the trapezius muscles were not accessible in the MRI environment).

Behavioral and Physiological Effects of Sevoflurane

All volunteers were awake and cooperative at baseline (modified OAA/S of 5 and Ramsay of 2) but were unresponsive at 1.2% sevoflurane (modified OAA/S of 0 and Ramsay of 6), consistent with the definition of general anesthesia.[29] The Modified OAA/S and Ramsay scores were different between the two groups ($p < 0.001$, Mann-Whitney U-test). The mean (± standard deviation) end-tidal sevoflurane concentrations were 0% (± 0%) and 1.2% (± 0.1%). There was a small but significant change in mean arterial carbon dioxide partial pressure ($PaCO_2$), from 42.1 (± 4.7) mmHg to 48.3 (± 6.0) mmHg ($p = 0.03$, Mann-Whitney U-test). Controls for CO_2 retention are included in the present analyses (see below).

Neuroimaging

Functional magnetic resonance imaging employed a Siemens 3T Trio scanner (Siemens, Erlangen, Germany) equipped with a standard 12-channel head coil. Structural imaging included one T1-weighted Magnetization Prepared Rapid Gradient Echo (MPRAGE: FOV 256 mm, TR 2400 ms, TE 3.16 ms, FA 8°, voxel size 1 mm isotropic, 176 slices) and one T2-weighted (FOV 256 mm, TR 6280 ms, TE 88 ms, FA 120°, voxel size 1 × 1 × 4 mm, 36 slices) scan. At least two 7.5 minute, T2*-weighted fMRI runs (FOV 256 mm, TR 2200 ms, TE 27 ms, FA 90°, 4 mm isotropic voxels, 36 slices/volume, 200 volumes/run) were acquired in each anesthetic condition. Participants were instructed to remain still and awake with eyes closed during fMRI.

Data Preprocessing

Image preprocessing proceeded as previously described[30] with the addition of fMRI image distortion correction using the FUGUE module in FSL.[31] Field maps were approximated using the technique described by Gholipour and colleagues.[32] Distortion correction and motion correction were combined in one resampling step to generate volumetric time-series in Talairach atlas space (3 × 3 × 3 mm cubic voxels). Each fMRI run was intensity normalized (one multiplicative constant applied to all voxels and all frames) to obtain a whole-brain mode value of 1000.[33] Owing to this normalization, BOLD signal amplitudes were interpretable both for purposes of frame censoring and evaluation of time-series covariance values.

Additional preprocessing in preparation for FC analyses included motion censoring based on the DVARS (temporal derivative of RMS BOLD signal across voxels) measure.[18,34] Motion censoring was computed before de-noising to avoid FC analyses of frames (volumes) with "cosmetically" improved DVARS values but retained artifact.[22] The DVARS censoring threshold was set at 0.4% root-mean-square frame-to-frame BOLD signal change[22] following 20 mm spatial pre-blur in each direction. Epochs containing fewer than 10 contiguous frames meeting the DVARS criterion were excluded from the functional connectivity computations. Of the 21 participants for whom BOLD fMRI was acquired, 15 were imaged at both 0% and after loss of consciousness induced by 1.2% sevoflurane. Of these, ten and nine, respectively, provided useable fMRI data in the 0% and 1.2%

sevoflurane conditions. Only 6 contributed useable data in both conditions. The fraction of uncensored data from each participant is listed as a table in Supplemental Digital Content 2. Rigorous quality assurance criteria resulted in a severe winnowing of the useable data but there was no statistically significant difference in the DVARS measures between the 0% and 1.2% sevoflurane data sets ($p = 0.62$, *t*-test). The distributions of these DVARS values are shown in Supplemental Digital Content 3. The fraction of uncensored frames in the analyzed data was 72.0% +/− 18.9% and 56.7% +/− 28.4%, respectively, in the 0% and 1.2% sevoflurane conditions. Head movement statistics (translation + rotation in units of root-mean-square mm), averaged over retained frames, were 0.35 ± 0.15 and 0.39 ± 0.18, respectively, for the 0% and 1.2% sevoflurane conditions.

Following motion censoring, the retained frames were made zero-mean within each voxel but the data were not otherwise temporally or spatially filtered. De-noising was accomplished using a strategy similar to CompCor.[35] Nuisance regressors were derived from white matter and ventricle masks, segmented in each individual using FreeSurfer,[36] then spatially resampled in register with the functional data. Nuisance regressors also were extracted from voxels in the extra-axial CSF space exhibiting high (> 2.5%) temporal standard deviation. Additional nuisance regressors were derived from rigid body head motion correction, the global signal (GS) averaged over the whole brain, and the GS temporal derivative.

Functional Connectivity Analyses

Our analysis includes conventional computation of FC using Pearson correlation.[37] The Pearson correlation coefficient is a unitless quantity not sensitive to signal amplitude. Previous observations suggest that anesthetic agents affect the amplitude of intrinsic activity more than its correlation structure.[38,39] Accordingly, we also report covariance analyses of BOLD time-series, in which sensitivity to the amplitude of BOLD fluctuations is retained. Algebraic formulae are given in the Appendix.

Functional connectivity (FC) was computed in terms of region of interest (ROI) pairs. ROIs were defined by dividing gray matter regions in atlas space into 9 × 9 × 9 mm cubes, discounting any cubes containing fewer than 50% gray matter voxels.[40] Each ROI was assigned to one of seven resting state networks (RSNs).[41] Only ROIs with over a 95% probability of belonging to one of these networks were retained in the analysis. A map of the ROIs and their network assignments is shown in Supplemental Digital Content 4, panel A. These network assignments were used to evaluate sevoflurane effects within particular functional systems. Additional FC analyses were computed in terms of voxelwise Pearson correlations with time-series extracted from specific regions of interest, e.g., the whole thalamus region in Supplemental Digital Content 4, panel B. Pearson correlations were Fisher z-transformed prior to averaging and statistical significance testing.

Statistical Analysis

Two-tailed *t*-tests were used to compare behavioral, physiologic, and FC analyses. Non-parametric Mann-Whitney *U* tests were used for hypothesis testing of covariance estimates. These statistical tests, as well as correlation and covariance analyses, were performed using

custom-written scripts implemented on Matlab (Mathworks, Natick, MA). As only 6 participants provided usable data in both conditions, all group-level significance testing reported in the main text was based on unpaired comparisons. Bonferroni corrections were applied to correct for multiple comparisons.

Results

Resting state fMRI Intracortical Functional Connectivity

Correlation and covariance matrices corresponding to 0% and 1.2% sevoflurane are shown in figure 1. All networks showed quantitative reductions of functional connectivity (FC) at 1.2% sevoflurane but only differences in the default mode network (DMN) and the ventral attention network (VAN) (fig. 1C) remained significant ($p < 0.05$, t-tests) after correction for multiple comparisons. The DMN is associated with social cognition and episodic memory and includes midline frontal and parietal structures.[42] In contrast, the VAN is involved in orienting to the external environment and includes anterior insula and anterior cingulate cortex.[43] Cognitive functions represented in both the DMN and VAN are considered more fully below (see Discussion). Compared to correlation analysis (figs. 1A and 1B), covariance analysis revealed marked widespread differences. Sevoflurane generally suppressed BOLD signal covariance and amplitudes within all RSNs (fig. 1F, *U* test $p < 10^{-8}$ for all comparisons, Bonferroni-corrected). We verified that the effects shown in figures 1C and 1F are found in a paired statistical analysis of the 6 subjects from whom data was acquired in both 0% and 1.2% sevoflurane conditions. These results are included for both correlation and covariance as bar graphs in Supplemental Digital Content 5.

Topographic Analysis of Sevoflurane Effects

Previous work suggests that propofol anesthesia[14] and slow-wave sleep[25,44] both reduce within-network BOLD correlations along the anterior-posterior brain axis. To examine this effect in our (motion-censored) data, FC maps were computed in the 0% and 1.2% sevoflurane conditions using seeds in the posterior cingulate cortex node of the DMN and fronto-polar nodes of the VAN (figure 2). The coordinates of these seeds have been previously reported.[45] A comparison across conditions revealed weakening of FC between anterior (medial prefrontal cortex, mPFC) and posterior (posterior cingulate cortex, PCC, fig. 2A) components of the DMN during sevoflurane anesthesia (figs. 2B and 2C). FC between the PCC and lateral parietal regions was preserved. Similarly, 1.2% sevoflurane reduced FC between the posterior parietal and the anterior portions of the VAN (figs. 2E and 2F).

Thalamocortical Functional Connectivity

Altered thalamic activity has been widely associated with changes in arousal state.[2,46,47] To examine the effects of sevoflurane on thalamocortical FC, we computed conventional, Pearson correlation maps using the entire thalamus region in Supplemental Digital Content 4 as a seed. This analysis showed that the primary effect of sevoflurane-induced unconsciousness was weakening of thalamocortical FC over much of the anterior aspect of the mesial surface of each hemisphere (figs. 3A and 3B). This anatomical territory encompasses portions of the DMN and VAN, the RSNs most altered in the analysis of

intracortical FC (fig. 1C). We therefore checked whether these thalamocortical effects were specific from the perspective of RSN assignment by computing the mean FC between the thalamus and the cortical representation of each RSN. Reduced thalamocortical FC was most pronounced in the DMN and VAN (fig. 3C, $p < 0.05$, paired *t*-tests).

The effects of 1.2% sevoflurane, assessed in terms of thalamocortical covariance, are shown in figures 4A and 4B, the format of which parallels figures 3A and 3B. Thalamocortical covariance values were generally reduced at 1.2% sevoflurane, especially over the mesial surface of the cerebral hemispheres. This result mirrors the pronounced reduction in BOLD signal amplitudes reflected in the intracortical covariance matrices (fig. 1F). Significant effects of sevoflurane were observed in ensemble measures (averages over within-RSN voxels) of the DMN, VAN, and dorsal attention networks (DAN) (fig. 4C, all $p < 0.05$, *U* test, Bonferroni corrected). This pattern of network specificity is similar to that shown in figure 3C except that the sensitivity of the covariance-based FC appears to be somewhat greater than correlation-based FC.

Functional Connectivity Analysis Without Motion Censoring

Intracortical FC analyses without quantitative motion censoring is demonstrated for BOLD signal correlation (fig. 5A–C) and covariance (fig. 5D–F), the format of which parallels fig. 1. Without motion censoring, the matrices are dominated by positive values reflecting widely shared artifactual variance.[22] No significant sevoflurane-related differences in within-network functional connectivity were revealed by the correlation analyses. Covariance analyses showed artifactual *increases* at 1.2% sevoflurane. These results stand in marked contrast to the results obtained with motion censoring (fig. 1), which include many more values near zero. Thus, scrupulous motion censoring is essential in studies of this type.

Controls for $PaCO_2$

The BOLD signal is sensitive to changes in retained carbon dioxide.[48] As sevoflurane anesthesia induces CO_2 retention,[49–51] we analyzed the extent to which changes in $PaCO_2$ account for the effects shown in figures 1C and 1F. This estimation was accomplished by regression of $PaCO_2$ from FC measures in each condition. $PaCO_2$ explained < 1% of the variance in (Fisher z-transformed) Pearson *r*-values. Regression of $PaCO_2$-dependent effects did not change the statistical significance of the sevoflurane effects in the correlation measures. Similarly, in the covariance analysis, $PaCO_2$ explained < 2% of the variance, also without affecting statistical significance of the sevoflurane effects.

Discussion

Summary of findings

We report a resting state fMRI study of humans rendered unresponsive by sevoflurane. The primary findings are that sevoflurane induces both a spatially widespread reduction in BOLD signal amplitude and also modest but specific reductions in intracortical and thalamocortical functional connectivity (FC) within the default mode (DMN) and ventral attention (VAN) networks. Our study differs from prior similar work in two principal characteristics: (i) Scrupulous attention to the problem of head-motion artifact constitutes a

major feature of the methodology. (ii) Covariance-based FC measures, which reflect BOLD signal amplitudes, are contrasted against conventional, correlation-based measures. We also demonstrate that, unless artifacts attributable to head motion are adequately addressed, sevoflurane effects in correlation-based FC measures are obscured (fig. 5C) and observed changes in the covariance structure of intrinsic activity are in the wrong direction (fig. 5F).

Correlation-based functional connectivity

The states of anesthetic-induced unconsciousness appear to resemble natural and pathologic reductions in consciousness. More specifically, disorders of consciousness,[23] absence epilepsy,[52,53] slow-wave sleep,[25,44] and propofol[14] and sevoflurane[39] anesthesia all are associated with reduced correlation between the posterior (posterior parietal precuneus cortex; PCC) and anterior (medial prefrontal cortex; mPFC) components of the DMN. Reduced anterior-posterior FC in the DMN has been related to impairments in memory consolidation,[54,55] which may relate to the amnesic effects of sevoflurane.[56] Reduced FC along the anterior-posterior axis of the DMN clearly is evident in our results (figs. 2B and 2C). This result is concordant with a recent study of sevoflurane anesthesia[39] but not others.[17,57] Our results (fig. 5C) indicate that insufficient attention to the problem of head motion artifact may account for these discrepancies.

We also observed significant reduction in FC along the anterior-posterior axis of the VAN (figs. 2E and 2F). Similar findings have been observed with propofol.[15,16] The VAN, as originally defined, includes the anterior cingulate, anterior insular, middle inferior frontal, and inferior frontal cortical regions.[43,58] Here, we also assign to the VAN parts of dorsolateral prefrontal cortex (DLPFC) and the temporal-parietal junction (TPJ).[41] Others have variably assigned these regions to the “external awareness network”[59] or the fronto-parietal control network.[60] Regardless of nomenclature, there is wide agreement that these regions mediate the capacity to respond to external events.[23,59–62] Our findings are also consistent with altered frontal-parietal FC reported in electroencephalographic studies of humans rendered unresponsive by sevoflurane, propofol, and other anesthetic agents.[4,63,64]

Altered thalamic activity is a well-established correlate of reduced arousal.[2,47,65–67] We observed focal reductions in FC between thalamus and midline cortical regions belonging to the DMN and VAN (fig. 3). In contrast, FC between thalamus and primary sensory areas was preserved (fig. 3). Experiments in rats anesthetized with sevoflurane indicate that pharmacologic excitation of medial (but not lateral) thalamus induces transient awakening.[68,69] Propofol has been reported to reduce cerebral blood flow specifically in the medial part of the thalamus.[67] It is therefore of considerable interest that the thalamic components of the DMN and the VAN are represented predominantly in midline nuclei.[70] Thus, our results support the hypothesis that sevoflurane preferentially acts on the medial thalamus in humans.

Covariance-based functional connectivity

Arguably, the most salient feature of the present results is the pervasive reduction in BOLD signal covariance at 1.2% sevoflurane (fig. 1F). We previously observed similar effects in a heterogeneous sample of pediatric epilepsy patients sedated with a variety of anesthetic

agents.[38] A similar finding, expressed in terms of voxelwise BOLD signal amplitudes, was recently reported by Huang and colleagues, who tested both sevoflurane and propofol.[39] That these effects have not been heretofore more widely recognized is understandable as the preponderance of resting state FC studies have been focused on delineating RSN topographies rather than measuring BOLD signal amplitudes.[71,72] Covariance measures have informed studies of stroke[73] and white matter injury in premature infants.[74] The present results indicate that the predominant effect of sevoflurane anesthesia on resting state fMRI signals is reduced amplitude, and consequently, reduced covariance.

This finding is entirely consistent with well-established results. Intrinsic signaling is the primary driver of spontaneous BOLD signal fluctuations[75,76] and also accounts for most of the brain's energy utilization.[77] In humans rendered unresponsive by sevoflurane, similar reductions from baseline have been reported in measures of global cerebral blood flow[78–80] and total cerebral metabolic consumption of glucose[79,81] and oxygen.[79,80] As coupling of global cerebral blood flow and metabolic consumption of oxygen and glucose remain intact[79], reduced amplitude of spontaneous resting state BOLD signal fluctuations can be understood as a correlate of reduced intrinsic activity.

Technical considerations in resting state fMRI studies of anesthetic states

Head motion, even of a sub-millimeter magnitude, generates significant artifact in fMRI[18,21] by interfering with the physics of echo-planar imaging ("spin-history" effects).[82] Such artifacts are relatively inconsequential in task-based fMRI because they are automatically reduced by response averaging.[83] However, this advantage does not apply to resting state fMRI.

We encountered unusually prevalent head motion even at 0% sevoflurane. The most likely explanation is discomfort attributable to respirations through a semi-closed breathing circuit. Anxiety related to anticipation of sedation also may have contributed. Subject motion during 0.6% sevoflurane sedation may be caused by paradoxical excitement[84] and by the inability of subjects to volitionally inhibit movement, as observed in prior studies of propofol sedation.[85,86] Almost none of the current fMRI data acquired at this state met our stringent quality assurance criteria. Useable data were acquired at 1.2% sevoflurane but data loss likely occurred due to intermittent agitation or partial airway obstruction. Thus, inhaled anesthetics present an especially challenging paradigm for resting state fMRI. This circumstance probably accounts for the fact that only a minority of reported studies listed in Supplemental Digital Content 1 used these agents (9/48, all sevoflurane).

Strategies for minimizing head motion artifact depend on functional connectivity methodology. With independent components analysis, it is possible to reject selected spatial components identified as artifact.[87] In seed-based correlation analysis, the principal strategy is regression of nuisance waveforms[35], as in the present work. However, regression of nuisance waveforms, including waveforms derived from retrospective motion correction, may be insufficient in seed-based analyses, depending on the prevalence of head motion. Even exclusion of fMRI data on the basis of mm-scale movements may not be sufficient. To obtain meaningful results in high-motion subjects, exclusion of corrupted volumes (frames) from the FC computations may be required.[18,22] Most of the reports listed in Supplemental

Digital Content 1 omit quantitative estimates of the prevalence and magnitude of head motion, thereby making it difficult to determine the reliability of reported FC results.

Carbon dioxide retention during sedation has the potential to alter FC. In this context, it is important to distinguish between moment-to-moment fluctuations in $PaCO_2$, which directly generate artifactual BOLD signal correlations,[48,88] from FC alterations induced by sustained changes in $PaCO_2$.[89,90] Less than one-third of the studies listed in Supplemental Digital Content 1 report surrogate measures of arterial CO_2. Propofol has been reported to induce 6–10 mmHg increases in $PaCO_2$[14] or end-tidal CO2 ($EtCO_2$).[37,85,86] These perturbations are comparable to the mild hypercapnia observed in our study (6 mmHg on average). More intense hypercapnia, e.g., 8–10 mmHg induced by 5% inhaled CO_2, has been reported to slightly reduce FC and BOLD signal amplitudes in the DMN.[90] Critically, we determined that run-to-run changes in $PaCO_2$ negligibly accounted for measured changes in FC (2% maximum explained variance).

Limitations and caveats

The primary limitation of the present study is the relatively small sample size (10 and 9, subjects respectively, at 0% and 1.2% sevoflurane). However, our study is not atypical in this regard compared to those in Supplemental Digital Content 1. It is worth emphasizing that studies of this type are exceedingly difficult because of the requirement for MRI-compatible ancillary equipment, limited participant tolerance for anesthetic-induced unconsciousness, and the high prevalence of subject motion.

Conclusions

The primary effect of sevoflurane-induced unconsciousness is diffuse reduction in BOLD signal amplitude consistent with widespread attenuation of neural activity. In addition, a modest degree of focality also is observed, in particular, reduced functional connectivity in distributed brain networks associated with episodic memory and orienting to environmental stimuli.

Supplementary Material

Refer to Web version on PubMed Central for supplementary material.

Acknowledgements

The authors thank Biyu He, Ph.D. (National Institute of Neurological Disorders and Stroke, Bethesda, MD, USA) and Eric Leuthardt, M.D. (Washington University School of Medicine, St. Louis, MO, USA) for discussion leading to the development of the project. We thank Jane Blood, B.S., R.N. (Washington University School of Medicine, St. Louis, MO, USA), Danielle Tallchief, R.N. (Washington University School of Medicine, St. Louis, MO, USA), and Kristin Kraus, B.S.N., R.N. (Washington University School of Medicine, St. Louis, MO, USA) for nursing support. We thank Tracy Nolan, B.S. (Washington University School of Medicine, St. Louis, MO, USA) for technical support. We thank Chris Smyser, M.D., M.Sc. (Washington University School of Medicine, St. Louis, MO, USA) for comments on the manuscript.

Funding: Foundation for Anesthesia Education and Research (Schaumburg, IL, USA) /Society for Neuroanesthesia and Critical Care (Richmond, VA, USA) Mentored Research Training Grant (BAP); National Institute of General Medical Sciences (Bethesda, MD, USA) Grant UL1 RR024992 (BAP), National Institute of General Medical Sciences (Bethesda, MD, USA) Grant U25 MH071279-01 (BAP), National Institute of Mental Health (Bethesda, MD, USA) Grant F30 MH106253 (AM), National Institute of Neurological Disorders and Stroke (Bethesda, MD,

USA) Grant P30 NS-048056 (AZS), The Washington University Department of Anesthesiology (St. Louis, MO, USA) (BAP), Mallinckrodt Institute of Radiology (St. Louis, MO, USA) (MER), and the McDonnell Center for Systems Neuroscience (St. Louis, MO, USA) (MER).

References

1. Franks NP. General anaesthesia: from molecular targets to neuronal pathways of sleep and arousal. Nat Rev Neurosci. 2008; 9:370–386. [PubMed: 18425091]
2. Alkire MT, Hudetz AG, Tononi G. Consciousness and anesthesia. Science. 2008; 322:876–880. [PubMed: 18988836]
3. Imas OA, Ropella KM, Ward BD, Wood JD, Hudetz AG. Volatile anesthetics disrupt frontal-posterior recurrent information transfer at gamma frequencies in rat. Neurosci Lett. 2005; 387:145–150. [PubMed: 16019145]
4. Lee U, Ku S, Noh G, Baek S, Choi B, Mashour GA. Disruption of frontal-parietal communication by ketamine, propofol, and sevoflurane. Anesthesiology. 2013; 118:1264–1275. [PubMed: 23695090]
5. Ogawa S, Lee TM, Nayak AS, Glynn P. Oxygenation-sensitive contrast in magnetic resonance image of rodent brain at high magnetic fields. Magn Reson Med. 1990; 14:68–78. [PubMed: 2161986]
6. Magri C, Schridde U, Murayama Y, Panzeri S, Logothetis NK. The amplitude and timing of the BOLD signal reflects the relationship between local field potential power at different frequencies. J Neurosci. 2012; 32:1395–1407. [PubMed: 22279224]
7. Liu TT, Frank LR, Wong EC, Buxton RB. Detection power, estimation efficiency, and predictability in event-related fMRI. Neuroimage. 2001; 13:759–773. [PubMed: 11305903]
8. Fox MD, Greicius M. Clinical applications of resting state functional connectivity. Frontiers in systems neuroscience. 2010; 4:19. [PubMed: 20592951]
9. Biswal B, Yetkin FZ, Haughton VM, Hyde JS. Functional connectivity in the motor cortex of resting human brain using echo-planar MRI. Magn Reson Med. 1995; 34:537–541. [PubMed: 8524021]
10. Beckmann CF, DeLuca M, Devlin JT, Smith SM. Investigations into resting-state connectivity using independent component analysis. Philos Trans R Soc Lond B Biol Sci. 2005; 360:1001–1013. [PubMed: 16087444]
11. Cordes D, Haughton VM, Arfanakis K, Wendt GJ, Turski PA, Moritz CH, Quigley MA, Meyerand ME. Mapping functionally related regions of brain with functional connectivity MR imaging. AJNR. American journal of neuroradiology. 2000; 21:1636–1644. [PubMed: 11039342]
12. Smith SM, Fox PT, Miller KL, Glahn DC, Fox PM, Mackay CE, Filippini N, Watkins KE, Toro R, Laird AR, Beckmann CF. Correspondence of the brain's functional architecture during activation and rest. Proceedings of the National Academy of Sciences of the United States of America. 2009; 106:13040–13045. [PubMed: 19620724]
13. Kiviniemi V, Jauhiainen J, Tervonen O, Paakko E, Oikarinen J, Vainionpaa V, Rantala H, Biswal B. Slow vasomotor fluctuation in fMRI of anesthetized child brain. Magn Reson Med. 2000; 44:373–378. [PubMed: 10975887]
14. Boveroux P, Vanhaudenhuyse A, Bruno MA, Noirhomme Q, Lauwick S, Luxen A, Degueldre C, Plenevaux A, Schnakers C, Phillips C, Brichant JF, Bonhomme V, Maquet P, Greicius MD, Laureys S, Boly M. Breakdown of within- and between-network resting state functional magnetic resonance imaging connectivity during propofol-induced loss of consciousness. Anesthesiology. 2010; 113:1038–1053. [PubMed: 20885292]
15. Schrouff J, Perlbarg V, Boly M, Marrelec G, Boveroux P, Vanhaudenhuyse A, Bruno MA, Laureys S, Phillips C, Pelegrini-Issac M, Maquet P, Benali H. Brain functional integration decreases during propofol-induced loss of consciousness. Neuroimage. 2011; 57:198–205. [PubMed: 21524704]
16. Guldenmund P, Demertzi A, Boveroux P, Boly M, Vanhaudenhuyse A, Bruno MA, Gosseries O, Noirhomme Q, Brichant JF, Bonhomme V, Laureys S, Soddu A. Thalamus, brainstem and salience network connectivity changes during propofol-induced sedation and unconsciousness. Brain Connect. 2013; 3:273–285. [PubMed: 23547875]

17. Martuzzi R, Ramani R, Qiu M, Rajeevan N, Constable RT. Functional connectivity and alterations in baseline brain state in humans. Neuroimage. 2010; 49:823–834. [PubMed: 19631277]
18. Power JD, Barnes KA, Snyder AZ, Schlaggar BL, Petersen SE. Spurious but systematic correlations in functional connectivity MRI networks arise from subject motion. Neuroimage. 2012; 59:2142–2154. [PubMed: 22019881]
19. Satterthwaite TD, Wolf DH, Loughead J, Ruparel K, Elliott MA, Hakonarson H, Gur RC, Gur RE. Impact of in-scanner head motion on multiple measures of functional connectivity: relevance for studies of neurodevelopment in youth. Neuroimage. 2012; 60:623–632. [PubMed: 22233733]
20. Van Dijk KR, Sabuncu MR, Buckner RL. The influence of head motion on intrinsic functional connectivity MRI. Neuroimage. 2012; 59:431–438. [PubMed: 21810475]
21. Yan CG, Cheung B, Kelly C, Colcombe S, Craddock RC, Di Martino A, Li Q, Zuo XN, Castellanos FX, Milham MP. A comprehensive assessment of regional variation in the impact of head micromovements on functional connectomics. Neuroimage. 2013; 76:183–201. [PubMed: 23499792]
22. Power JD, Mitra A, Laumann TO, Snyder AZ, Schlaggar BL, Petersen SE. Methods to detect, characterize, and remove motion artifact in resting state fMRI. Neuroimage. 2014; 84:320–341. [PubMed: 23994314]
23. Boly M, Massimini M, Garrido MI, Gosseries O, Noirhomme Q, Laureys S, Soddu A. Brain connectivity in disorders of consciousness. Brain Connect. 2012; 2:1–10. [PubMed: 22512333]
24. Dang-Vu TT, Schabus M, Desseilles M, Albouy G, Boly M, Darsaud A, Gais S, Rauchs G, Sterpenich V, Vandewalle G, Carrier J, Moonen G, Balteau E, Degueldre C, Luxen A, Phillips C, Maquet P. Spontaneous neural activity during human slow wave sleep. Proc Natl Acad Sci U S A. 2008; 105:15160–15165. [PubMed: 18815373]
25. Samann PG, Wehrle R, Hoehn D, Spoormaker VI, Peters H, Tully C, Holsboer F, Czisch M. Development of the brain's default mode network from wakefulness to slow wave sleep. Cereb Cortex. 2011; 21:2082–2093. [PubMed: 21330468]
26. Nickalls RW, Mapleson WW. Age-related iso-MAC charts for isoflurane, sevoflurane and desflurane in man. Br J Anaesth. 2003; 91:170–174. [PubMed: 12878613]
27. Chernik DA, Gillings D, Laine H, Hendler J, Silver JM, Davidson AB, Schwam EM, Siegel JL. Validity and reliability of the Observer's Assessment of Alertness/Sedation Scale: study with intravenous midazolam. J Clin Psychopharmacol. 1990; 10:244–251. [PubMed: 2286697]
28. Ramsay MA, Savege TM, Simpson BR, Goodwin R. Controlled sedation with alphaxalone-alphadolone. Br Med J. 1974; 2:656–659. [PubMed: 4835444]
29. Continuum of Depth of Sedation: Definition of General Anesthesia and Levels of Sedation/Analgesia, American Society of Anesthesiologists, approved 1999, last amended 2014. http://www.asahq.org/~/media/Sites/ASAHQ/Files/Public/Resources/standards-guidelines/continuum-of-depth-of-sedation-definition-of-general-anesthesia-and-levels-of-sedation-analgesia.pdf.
30. Shulman GL, Pope DL, Astafiev SV, McAvoy MP, Snyder AZ, Corbetta M. Right hemisphere dominance during spatial selective attention and target detection occurs outside the dorsal frontoparietal network. The Journal of neuroscience : the official journal of the Society for Neuroscience. 2010; 30:3640–3651. [PubMed: 20219998]
31. Jenkinson M, Beckmann CF, Behrens TE, Woolrich MW, Smith SM. Fsl. Neuroimage. 2012; 62:782–790. [PubMed: 21979382]
32. Gholipour A, Kehtarnavaz N, Gopinath K, Briggs R, Panahi I. Average field map image template for Echo-Planar image analysis. Conf Proc IEEE Eng Med Biol Soc. 2008; 2008:94–97. [PubMed: 19162602]
33. Ojemann JG, Akbudak E, Snyder AZ, McKinstry RC, Raichle ME, Conturo TE. Anatomic localization and quantitative analysis of gradient refocused echo-planar fMRI susceptibility artifacts. Neuroimage. 1997; 6:156–167. [PubMed: 9344820]
34. Smyser CD, Inder TE, Shimony JS, Hill JE, Degnan AJ, Snyder AZ, Neil JJ. Longitudinal analysis of neural network development in preterm infants. Cereb Cortex. 2010; 20:2852–2862. [PubMed: 20237243]
35. Behzadi Y, Restom K, Liau J, Liu TT. A component based noise correction method (CompCor) for BOLD and perfusion based fMRI. Neuroimage. 2007; 37:90–101. [PubMed: 17560126]

36. Fischl B. FreeSurfer. Neuroimage. 2012; 62:774–781. [PubMed: 22248573]
37. Mhuircheartaigh RN, Rosenorn-Lanng D, Wise R, Jbabdi S, Rogers R, Tracey I. Cortical and subcortical connectivity changes during decreasing levels of consciousness in humans: a functional magnetic resonance imaging study using propofol. J Neurosci. 2010; 30:9095–9102. [PubMed: 20610743]
38. Pizoli CE, Shah MN, Snyder AZ, Shimony JS, Limbrick DD, Raichle ME, Schlaggar BL, Smyth MD. Resting-state activity in development and maintenance of normal brain function. Proc Natl Acad Sci U S A. 2011; 108:11638–11643. [PubMed: 21709227]
39. Huang Z, Wang Z, Zhang J, Dai R, Wu J, Li Y, Liang W, Mao Y, Yang Z, Holland G, Zhang J, Northoff G. Altered temporal variance and neural synchronization of spontaneous brain activity in anesthesia. Hum Brain Mapp. 2014; 35:5368–5378. [PubMed: 24867379]
40. Mitra A, Snyder AZ, Hacker CD, Raichle ME. Lag structure in resting state fMRI. J Neurophysiol. 2014; 111:2374–2391. [PubMed: 24598530]
41. Hacker CD, Laumann TO, Szrama NP, Baldassarre A, Snyder AZ, Leuthardt EC, Corbetta M. Resting state network estimation in individual subjects. Neuroimage. 2013; 82:616–633. [PubMed: 23735260]
42. Buckner RL, Andrews-Hanna JR, Schacter DL. The brain's default network: anatomy, function, and relevance to disease. Ann N Y Acad Sci. 2008; 1124:1–38. [PubMed: 18400922]
43. Corbetta M, Shulman GL. Control of goal-directed and stimulus-driven attention in the brain. Nat Rev Neurosci. 2002; 3:201–215. [PubMed: 11994752]
44. Horovitz SG, Braun AR, Carr WS, Picchioni D, Balkin TJ, Fukunaga M, Duyn JH. Decoupling of the brain's default mode network during deep sleep. Proc Natl Acad Sci U S A. 2009; 106:11376–11381. [PubMed: 19549821]
45. Brier MR, Thomas JB, Snyder AZ, Benzinger TL, Zhang D, Raichle ME, Holtzman DM, Morris JC, Ances BM. Loss of intranetwork and internetwork resting state functional connections with Alzheimer's disease progression. J Neurosci. 2012; 32:8890–8899. [PubMed: 22745490]
46. Gili T, Saxena N, Diukova A, Murphy K, Hall JE, Wise RG. The thalamus and brainstem act as key hubs in alterations of human brain network connectivity induced by mild propofol sedation. J Neurosci. 2013; 33:4024–4031. [PubMed: 23447611]
47. Mashour GA, Alkire MT. Consciousness, anesthesia, and the thalamocortical system. Anesthesiology. 2013; 118:13–15. [PubMed: 23208518]
48. Wise RG, Ide K, Poulin MJ, Tracey I. Resting fluctuations in arterial carbon dioxide induce significant low frequency variations in BOLD signal. Neuroimage. 2004; 21:1652–1664. [PubMed: 15050588]
49. Doi M, Ikeda K. Respiratory effects of sevoflurane. Anesth Analg. 1987; 66:241–244. [PubMed: 3826666]
50. Salihoglu Z, Demiroluk S, Demirkiran O, Emin I, Kose Y. Effects of sevoflurane, propofol and position changes on respiratory mechanics. Middle East J Anesthesiol. 2004; 17:811–818. [PubMed: 15449741]
51. Sen P, Izdes S, But A. Effects of sevoflurane and propofol anaesthesia on cerebral oxygenation during normocapnia and mild hypercapnia: a pilot study. Br J Anaesth. 2013; 110:318–319. [PubMed: 23319678]
52. Bai X, Vestal M, Berman R, Negishi M, Spann M, Vega C, Desalvo M, Novotny EJ, Constable RT, Blumenfeld H. Dynamic time course of typical childhood absence seizures: EEG, behavior, and functional magnetic resonance imaging. J Neurosci. 2010; 30:5884–5893. [PubMed: 20427649]
53. Laufs H, Lengler U, Hamandi K, Kleinschmidt A, Krakow K. Linking generalized spike-and-wave discharges and resting state brain activity by using EEG/fMRI in a patient with absence seizures. Epilepsia. 2006; 47:444–448. [PubMed: 16499775]
54. Buckner RL, Carroll DC. Self-projection and the brain. Trends Cogn Sci. 2007; 11:49–57. [PubMed: 17188554]
55. Spreng RN, Grady CL. Patterns of brain activity supporting autobiographical memory, prospection, and theory of mind, and their relationship to the default mode network. J Cogn Neurosci. 2010; 22:1112–1123. [PubMed: 19580387]

56. Kerssens C, Hamann S, Peltier S, Hu XP, Byas-Smith MG, Sebel PS. Attenuated brain response to auditory word stimulation with sevoflurane: a functional magnetic resonance imaging study in humans. Anesthesiology. 2005; 103:11–19. [PubMed: 15983451]
57. Martuzzi R, Ramani R, Qiu M, Shen X, Papademetris X, Constable RT. A whole-brain voxel based measure of intrinsic connectivity contrast reveals local changes in tissue connectivity with anesthetic without a priori assumptions on thresholds or regions of interest. Neuroimage. 2011; 58:1044–1050. [PubMed: 21763437]
58. Seeley WW, Menon V, Schatzberg AF, Keller J, Glover GH, Kenna H, Reiss AL, Greicius MD. Dissociable intrinsic connectivity networks for salience processing and executive control. J Neurosci. 2007; 27:2349–2356. [PubMed: 17329432]
59. Vanhaudenhuyse A, Demertzi A, Schabus M, Noirhomme Q, Bredart S, Boly M, Phillips C, Soddu A, Luxen A, Moonen G, Laureys S. Two distinct neuronal networks mediate the awareness of environment and of self. J Cogn Neurosci. 2011; 23:570–578. [PubMed: 20515407]
60. Dosenbach NU, Fair DA, Miezin FM, Cohen AL, Wenger KK, Dosenbach RA, Fox MD, Snyder AZ, Vincent JL, Raichle ME, Schlaggar BL, Petersen SE. Distinct brain networks for adaptive and stable task control in humans. Proc Natl Acad Sci U S A. 2007; 104:11073–11078. [PubMed: 17576922]
61. Vincent JL, Kahn I, Snyder AZ, Raichle ME, Buckner RL. Evidence for a frontoparietal control system revealed by intrinsic functional connectivity. J Neurophysiol. 2008; 100:3328–3342. [PubMed: 18799601]
62. Demertzi A, Soddu A, Laureys S. Consciousness supporting networks. Curr Opin Neurobiol. 2013; 23:239–244. [PubMed: 23273731]
63. Ku SW, Lee U, Noh GJ, Jun IG, Mashour GA. Preferential inhibition of frontal-to-parietal feedback connectivity is a neurophysiologic correlate of general anesthesia in surgical patients. PLoS One. 2011; 6:e25155. [PubMed: 21998638]
64. Lee U, Kim S, Noh GJ, Choi BM, Hwang E, Mashour GA. The directionality and functional organization of frontoparietal connectivity during consciousness and anesthesia in humans. Conscious Cogn. 2009; 18:1069–1078. [PubMed: 19443244]
65. Alkire MT, Haier RJ, Fallon JH. Toward a unified theory of narcosis: brain imaging evidence for a thalamocortical switch as the neurophysiologic basis of anesthetic-induced unconsciousness. Conscious Cogn. 2000; 9:370–386. [PubMed: 10993665]
66. Alkire MT, Miller J. General anesthesia and the neural correlates of consciousness. Prog Brain Res. 2005; 150:229–244. [PubMed: 16186027]
67. Fiset P, Paus T, Daloze T, Plourde G, Meuret P, Bonhomme V, Hajj-Ali N, Backman SB, Evans AC. Brain mechanisms of propofol-induced loss of consciousness in humans: a positron emission tomographic study. J Neurosci. 1999; 19:5506–5513. [PubMed: 10377359]
68. Alkire MT, Asher CD, Franciscus AM, Hahn EL. Thalamic microinfusion of antibody to a voltage-gated potassium channel restores consciousness during anesthesia. Anesthesiology. 2009; 110:766–773. [PubMed: 19322942]
69. Alkire MT, McReynolds JR, Hahn EL, Trivedi AN. Thalamic microinjection of nicotine reverses sevoflurane-induced loss of righting reflex in the rat. Anesthesiology. 2007; 107:264–272. [PubMed: 17667571]
70. Zhang D, Snyder AZ, Fox MD, Sansbury MW, Shimony JS, Raichle ME. Intrinsic functional relations between human cerebral cortex and thalamus. J Neurophysiol. 2008; 100:1740–1748. [PubMed: 18701759]
71. Damoiseaux JS, Rombouts SA, Barkhof F, Scheltens P, Stam CJ, Smith SM, Beckmann CF. Consistent resting-state networks across healthy subjects. Proc Natl Acad Sci U S A. 2006; 103:13848–13853. [PubMed: 16945915]
72. Shehzad Z, Kelly AM, Reiss PT, Gee DG, Gotimer K, Uddin LQ, Lee SH, Margulies DS, Roy AK, Biswal BB, Petkova E, Castellanos FX, Milham MP. The resting brain: unconstrained yet reliable. Cerebral cortex. 2009; 19:2209–2229. [PubMed: 19221144]
73. Varoquaux G, Baronnet F, Kleinschmidt A, Fillard P, Thirion B. Detection of brain functional-connectivity difference in post-stroke patients using group-level covariance modeling. Medical

image computing and computer-assisted intervention : MICCAI. International Conference on Medical Image Computing and Computer-Assisted Intervention. 2010; 13:200–208.

74. Smyser CD, Snyder AZ, Shimony JS, Blazey TM, Inder TE, Neil JJ. Effects of white matter injury on resting state FMRI measures in prematurely born infants. PLoS One. 2013; 8:e68098. [PubMed: 23874510]
75. Llinas R, Ribary U, Contreras D, Pedroarena C. The neuronal basis for consciousness. Philos Trans R Soc Lond B Biol Sci. 1998; 353:1841–1849. [PubMed: 9854256]
76. Raichle ME. The restless brain. Brain Connect. 2011; 1:3–12. [PubMed: 22432951]
77. Raichle ME, Mintun MA. Brain work and brain imaging. Annu Rev Neurosci. 2006; 29:449–476. [PubMed: 16776593]
78. Kaisti KK, Metsahonkala L, Teras M, Oikonen V, Aalto S, Jaaskelainen S, Hinkka S, Scheinin H. Effects of surgical levels of propofol and sevoflurane anesthesia on cerebral blood flow in healthy subjects studied with positron emission tomography. Anesthesiology. 2002; 96:1358–1370. [PubMed: 12170048]
79. Mielck F, Stephan H, Weyland A, Sonntag H. Effects of one minimum alveolar anesthetic concentration sevoflurane on cerebral metabolism, blood flow, and CO2 reactivity in cardiac patients. Anesth Analg. 1999; 89:364–369. [PubMed: 10439749]
80. Kaisti KK, Langsjo JW, Aalto S, Oikonen V, Sipila H, Teras M, Hinkka S, Metsahonkala L, Scheinin H. Effects of sevoflurane, propofol, and adjunct nitrous oxide on regional cerebral blood flow, oxygen consumption, and blood volume in humans. Anesthesiology. 2003; 99:603–613. [PubMed: 12960544]
81. Schlunzen L, Juul N, Hansen KV, Gjedde A, Cold GE. Regional cerebral glucose metabolism during sevoflurane anaesthesia in healthy subjects studied with positron emission tomography. Acta Anaesthesiol Scand. 2010; 54:603–609. [PubMed: 20085540]
82. Friston KJ, Williams S, Howard R, Frackowiak RS, Turner R. Movement-related effects in fMRI time-series. Magn Reson Med. 1996; 35:346–355. [PubMed: 8699946]
83. Siegel JS, Power JD, Dubis JW, Vogel AC, Church JA, Schlaggar BL, Petersen SE. Statistical improvements in functional magnetic resonance imaging analyses produced by censoring high-motion data points. Hum Brain Mapp. 2014; 35:1981–1996. [PubMed: 23861343]
84. Fulton SA, Mullen KD. Completion of upper endoscopic procedures despite paradoxical reaction to midazolam: a role for flumazenil? Am J Gastroenterol. 2000; 95:809–811. [PubMed: 10710082]
85. Jordan D, Ilg R, Riedl V, Schorer A, Grimberg S, Neufang S, Omerovic A, Berger S, Untergehrer G, Preibisch C, Schulz E, Schuster T, Schroter M, Spoormaker V, Zimmer C, Hemmer B, Wohlschlager A, Kochs EF, Schneider G. Simultaneous electroencephalographic and functional magnetic resonance imaging indicate impaired cortical top-down processing in association with anesthetic-induced unconsciousness. Anesthesiology. 2013; 119:1031–1042. [PubMed: 23969561]
86. Schroter MS, Spoormaker VI, Schorer A, Wohlschlager A, Czisch M, Kochs EF, Zimmer C, Hemmer B, Schneider G, Jordan D, Ilg R. Spatiotemporal reconfiguration of large-scale brain functional networks during propofol-induced loss of consciousness. J Neurosci. 2012; 32:12832–12840. [PubMed: 22973006]
87. Tohka J, Foerde K, Aron AR, Tom SM, Toga AW, Poldrack RA. Automatic independent component labeling for artifact removal in fMRI. Neuroimage. 2008; 39:1227–1245. [PubMed: 18042495]
88. Chang C, Glover GH. Relationship between respiration, end-tidal CO2, and BOLD signals in resting-state fMRI. Neuroimage. 2009; 47:1381–1393. [PubMed: 19393322]
89. Madjar C, Gauthier CJ, Bellec P, Birn RM, Brooks JC, Hoge RD. Task-related BOLD responses and resting-state functional connectivity during physiological clamping of end-tidal CO(2). Neuroimage. 2012; 61:41–49. [PubMed: 22418394]
90. Xu F, Uh J, Brier MR, Hart J Jr, Yezhuvath US, Gu H, Yang Y, Lu H. The influence of carbon dioxide on brain activity and metabolism in conscious humans. J Cereb Blood Flow Metab. 2011; 31:58–67. [PubMed: 20842164]
91. Box, GEP.; Jenkins, GM.; Reinsel, GC. Time series analysis : forecasting and control. 4th edition. Hoboken, N.J.: J. Wiley; 2008.

Appendix

Mathematic Note

Our resting state fMRI preprocessing stream causes the time-average of the signal value at each voxel to be zero mean. Thus,

$$\overline{f}_i = \frac{1}{T}\int_0^T f_i(t)dt = 0,$$

where $f_i(t)$ is the signal averaged over region of interest i. Hence, all signals can be viewed as time-dependent fluctuations about a mean of zero. Standard covariance and correlation formulae[91] are discussed below.

The covariance between time-dependent signals, $f_i(t)$ and $f_j(t)$, is

$$c_{ij} = \frac{1}{T}\int_0^T f_i(t) f_j(t)dt.$$

The Pearson product-moment correlation is

$$r_{ij} = \frac{c_{ij}}{\sqrt{\sigma_i^2 \sigma_j^2}} = c_{ij}/(\sigma_i \sigma_j), \text{where}$$

$$\sigma_i^2 = c_{ii} = \frac{1}{T}\int_0^T f_i^2(t)dt.$$

Thus, correlation is covariance normalized by root mean square (rms) deviation (σ). N.B.: the signal temporal s.d. is σ. Correlation becomes undefined as the s.d. of either of the two involved signals approaches zero. r_{ij} is a unit-less scalar confined to the range (−1, +1). c_{ij} has units (fMRI signal)^2 and can assume any value in the range (−221E;, +∞).

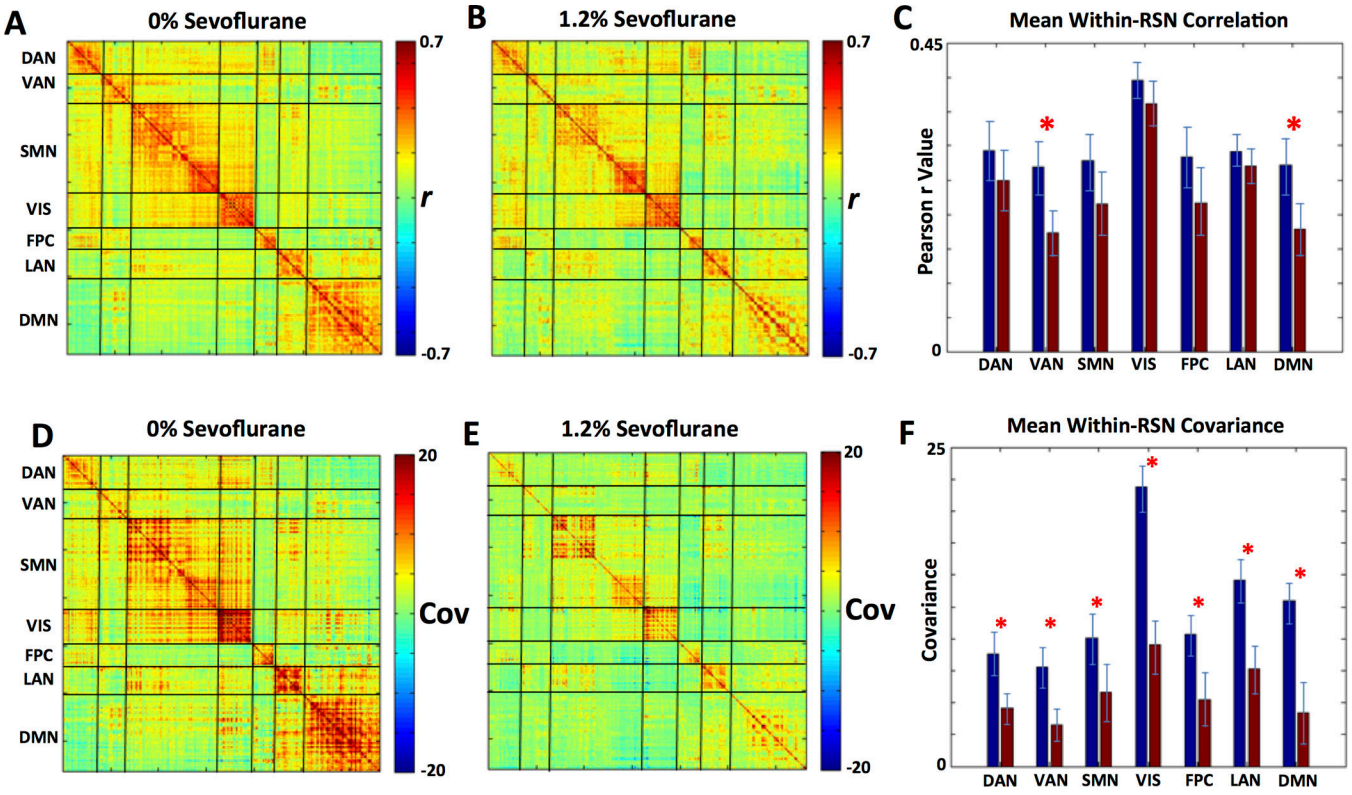

Fig. 1. Intracortical functional connectivity

The matrices display group-averaged, Fisher z-transformed Pearson correlations (A–C) and covariance (D–E) computed for pairs of BOLD signals extracted from all regions of interest (ROIs). The ROIs are 9 × 9 × 9 mm cubes defined over all gray matter in Talairach atlas space.[40] The ROIs are ordered in each matrix by resting state network (RSN) affiliation illustrated in Supplemental Digital Content 4. A and D: 0% sevoflurane (10 subjects). B and E: 1.2% sevoflurane (9 subjects). Bar plots represent within-network mean correlations averaged over matrix diagonal blocks, i.e., "RSN composite scores".[45] Blue: 0% sevoflurane. Red: 1.2% sevoflurane. C: Conventional correlation. Red stars in C indicate significant sevoflurane effects ($p < 0.05$, two-tailed *t*-test, multiple comparisons [N = 7 RSNs] corrected). F: Covariance. Red stars indicate significant differences in intra-network FC ($p < 0.05$, two-tailed *U* test, multiple comparisons [N = 7 RSNs] corrected).

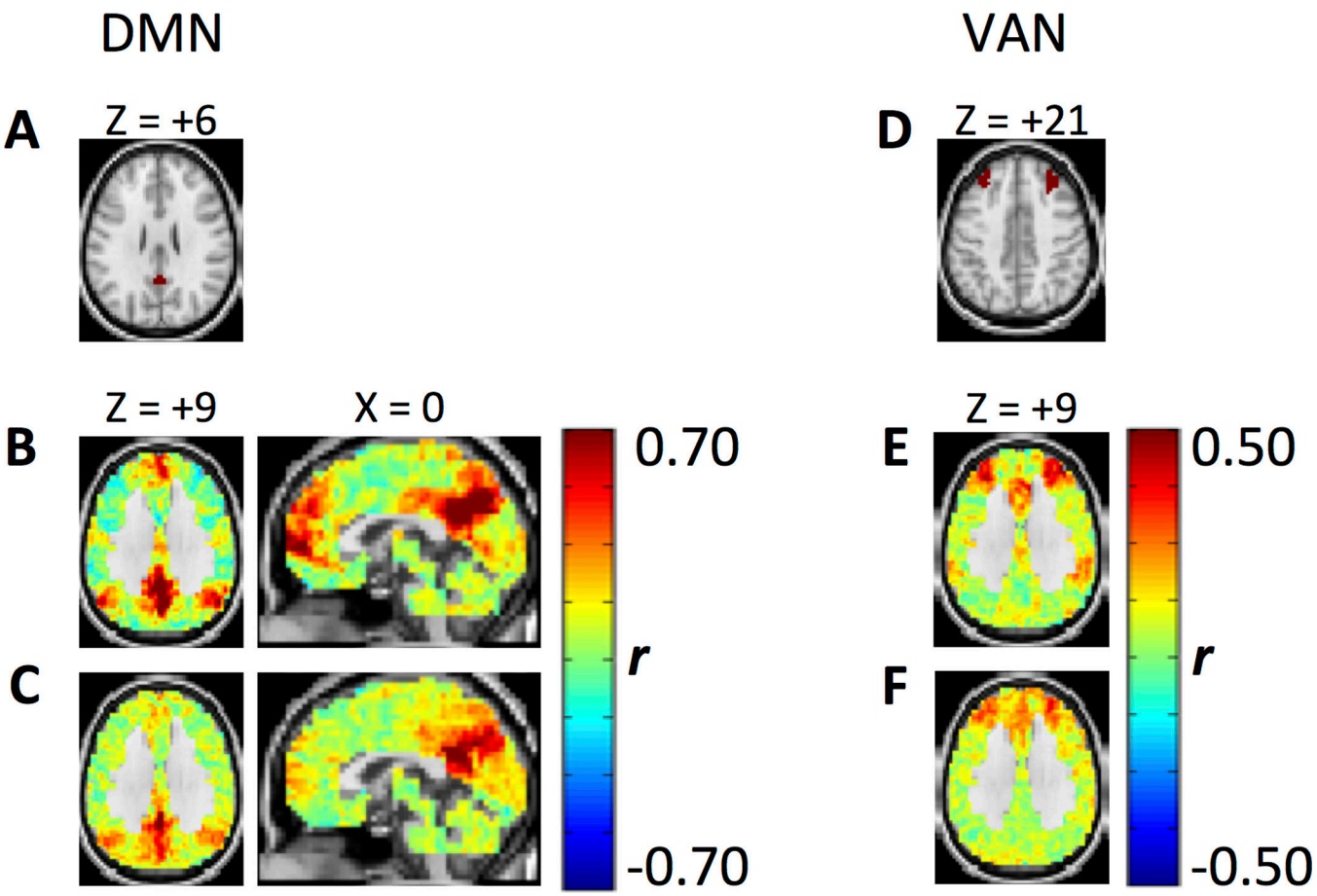

Fig. 2. Conventional seed-based correlation maps

The plotted quantity is the (Fisher z-transformed) correlation coefficient. A: Seed region in the posterior cingulate/precuneus cortex (PCC). B: correlation map at 0% sevoflurane. C: correlation map at 1.2% sevoflurane. Note reduced functional connectivity (FC) along the anterior-posterior axis in the anesthetized condition with relatively preserved FC between the PCC and lateral parietal nodes of the default mode network (DMN). D: Seed region, bilaterally defined in fronto-polar cortex. E: correlation map at 0% sevoflurane. F: correlation map at 1.2% sevoflurane. Note reduced FC between fronto-polar cortex and posterior nodes of the ventral attention network (VAN) in the anesthetized condition with relatively preserved FC between fronto-polar and dorsal cingulate cortex. Talairach coordinates next to maps represent plane of section. Seed Talairach coordinates are previously reported.[40]

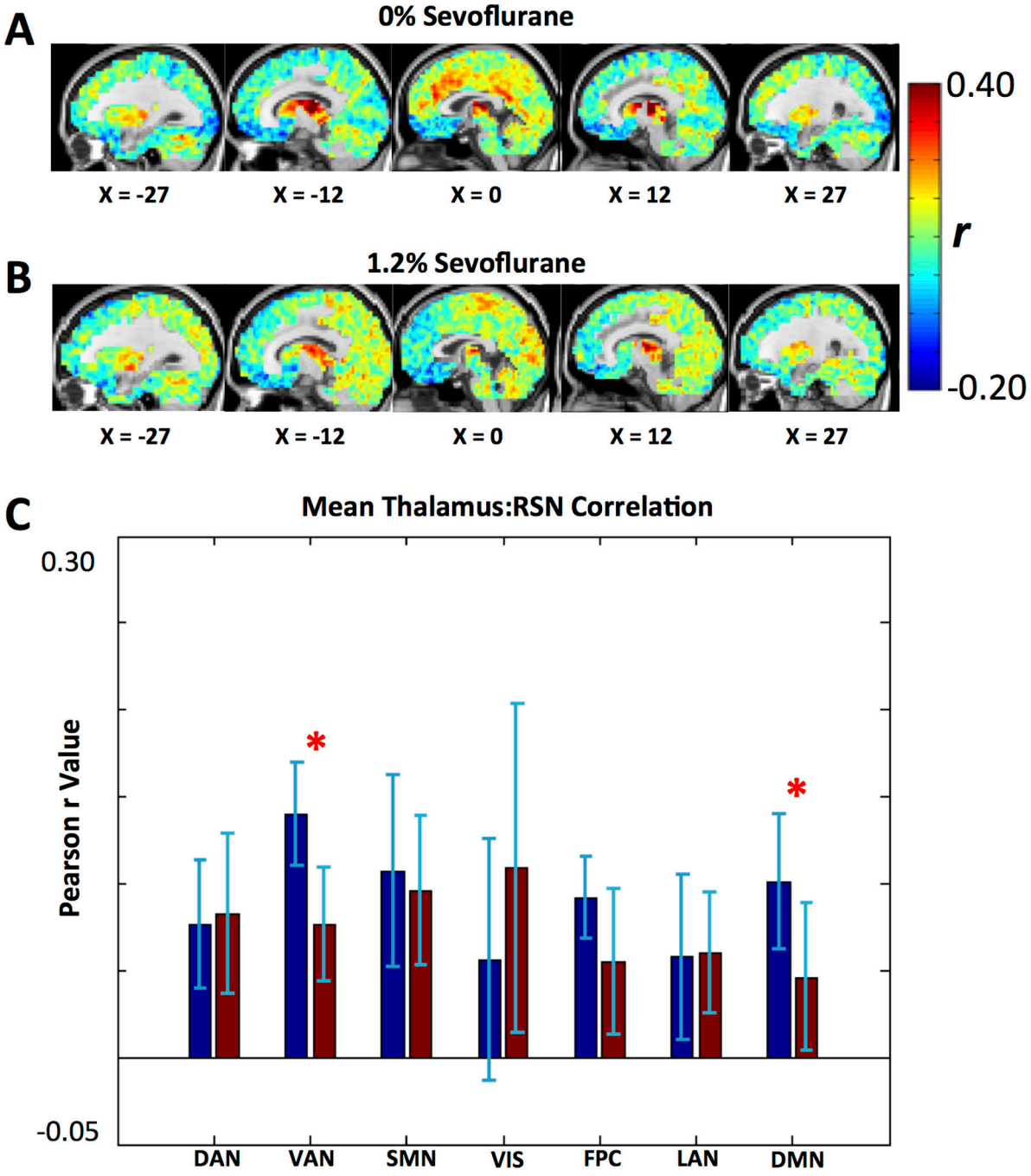

Fig. 3. Conventional thalamocortical functional connectivity

The seed is the whole-thalamus shown in Supplemental Digital Content 4. A: 0% sevoflurane. B: 1.2% sevoflurane. Note reduced thalamocortical functional connectivity (FC) over the mesial surface of each hemisphere (X = 0) in the anesthetized condition. C: Ensemble measures of thalamocortical FC in the 7 resting state networks (RSNs) illustrated in Supplemental Digital Content 4. The plotted quantity is the (Fisher z-transformed) correlation coefficient averaged over cortical voxels assigned to each RSN ("ensemble measure"). Blue and red bars indicate 0% and 1.2% sevoflurane, as in fig. 1. Red stars

indicate significant sevoflurane effects ($p < 0.05$, two-tailed *t*-test, Bonferroni-corrected). Note strongest effect of anesthesia in the default mode network (DMN) and the ventral attention network (VAN).

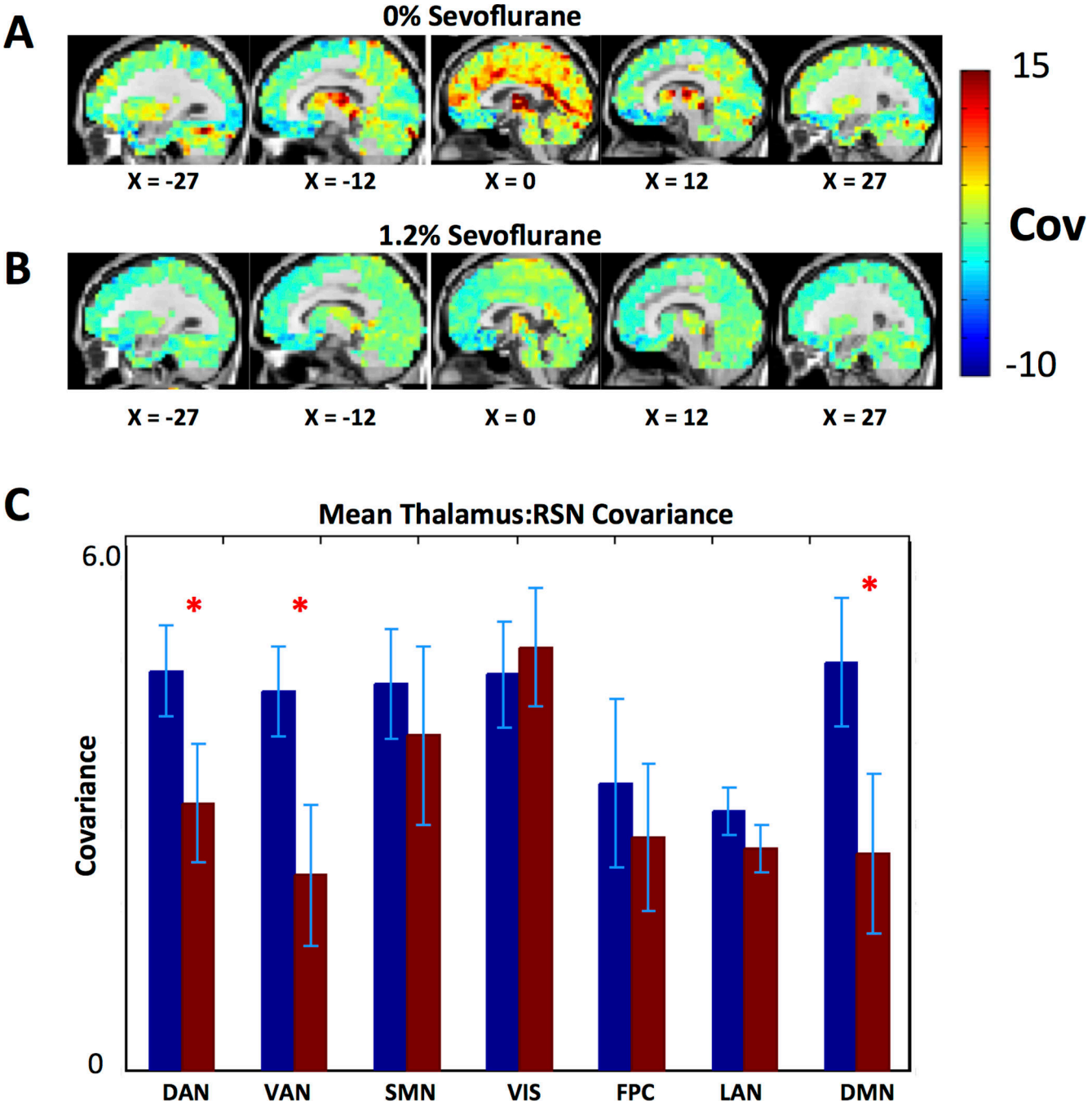

Fig. 4. Covariance-based thalamocortical functional connectivity

The format of this figure is identical to that of fig. 3. A and B show covariance-based functional connectivity (FC) maps computed using the whole-thalamus seed shown in Supplemental Digital Content 4. Note reduction in covariance between thalamus and anterior midline structures (X = 0) in the anesthetized condition. C: Ensemble measures of thalamocortical covariance values averaged over cortical voxels assigned to the 7 resting state networks (RSNs) illustrated in Supplemental Digital Content 4. Blue: 0% sevoflurane. Red: 1.2% sevoflurane. Note significant reductions in covariance-based thalamocortical FC

in the dorsal attention network (DAN), ventral attention network (VAN), and default mode network (DMN) (red stars, $p < 0.05$, *U* test, Bonferroni-corrected).

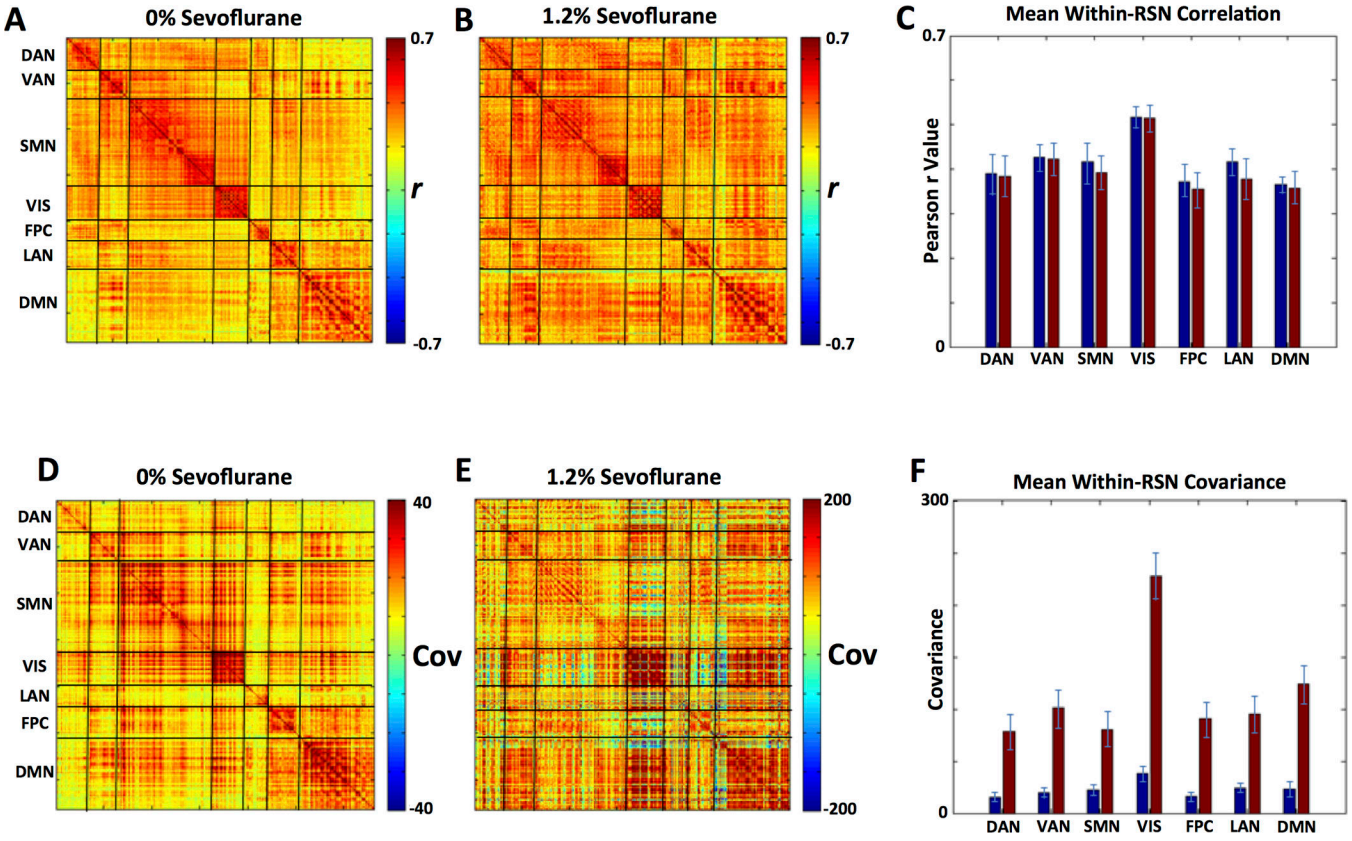

Fig. 5. Effect of omitting motion censoring in data acquired during sevoflurane anesthesia

The format of this figure is identical to that of fig. 1 but display analyses of data that have not undergone motion censoring. A and D: 0% sevoflurane. B and E: 1.2% sevoflurane. A–C: Correlation. D–F: Covariance. The bar plots are computed identically to those in fig. 1. Red stars are omitted in F as the observed differences are artifactual. Also note also different scales for covariance compared to figs. 1C and 1F.